Ductile Fracture of Carbon Steels: A Review

J. Pospiech

This paper presents an extensive survey of literature on the theory of deformation and failure of inhomogeneous materials. Literature concerning deformation and fracture of carbon steels also is reviewed.

Keywords
ductile fracture, carbon steels, deformation, inhomogeneous materials

1. Introduction

THE best utilization of deformability in cold-working processes translates into increased production, full use of available equipment capacity, and reduction of interannealing operations (Ref 1).

In order to know the deformability of materials such as steels, one must know the mechanisms involved in deformation and fracture of nonhomogeneous materials, as well as the plastic fracture criterion. This requires use of metallographic examination techniques.

2. Theory of Deformation of Nonhomogeneous Materials

2.1 *Nucleation of Voids*

This work utilized the theories of elasticity and plasticity covering the range of deformation and failure of nonhomogeneous materials. It is usually assumed that such materials consist of a matrix having good plastic properties and second-phase particles embedded in the matrix that either deform elastically or do not deform. Consider the deformation of such a composite system. The properties of the matrix and the second-phase particles are different (for example, they have different elastic constants), the matrix deforms first and then the particles change their initial shape. Since, according to the assumption, the second-phase particles undergo only elastic deformation or else do not undergo any deformation when the matrix enters the region of plastic deformation, there is considerable, and increasing, difference in the amount of deformation incurred by both constituents. This difference causes stress and strain concentrations and leads to generation of the secondary state of stress, which differs from the applied state of stress. The extent of these phenomena depends on the amount, distribution, shape, orientation relative to the external field of stress (this being of special importance for materials with a fibrous structure), and properties of the second-phase particles (in relation to the matrix). The local stress and strain concentrations, growing with the macroscopic deformation, are the cause of microcrack formation.

All theories of the nucleation of voids have been reviewed in Ref 2, and it has been stated (Ref 2, 3) that second-phase particles and inclusions in plastic matrices initiate voids either by interfacial decohesion or by fracturing of the particle. Although a somewhat higher incidence of interfacial decohesion occurs for equiaxed particles and internal fracturing for elongated particles, fracturing of equiaxed particles is also widely observed. Two conditions must be satisfied for crack nucleation at low temperature where diffusion plays no role (Ref 3): (1) The local stress must reach the strength of the interface or the cohesive strength of the particle, and (2) it should be possible to release enough elastic energy from the unloaded regions traversed by the crack to make up for the surface energy of the void or microcrack (Ref 3). Tanaka et al. (Ref 4) have shown that the latter condition is almost always satisfied for particles with diameters greater than 250 Å. It can be concluded (Ref 2) that for very small particles with diameters much less than the critical diameter of 250 Å, where the energy criterion may not be satisfied even when local stresses reach the interfacial strength, stable cavities are difficult to form.

Opinions differ as to when voids are nucleated, although it can be assumed (Ref 3) that for oxides, carbides, and manganese sulfide inclusions, voids are present from the beginning. It should be remembered (Ref 5), however, that inclusions with very weak cohesion with the matrix will not directly form microcracks, but rather "holes." If the matrix is sufficiently ductile (e.g., ferrite), microcrack formation will be considerably retarded, and these holes will act as stresses raisers as long as critical strains and stresses are reached for creation of microcracks (Ref 5).

Many investigators have reported the presence or absence of a particle-size effect in void nucleation, although it appears that voids nucleate first from the large particles. Different explanations have been offered for this effect (Ref 3).

In addition to the qualitative aspect, the possibility of quantitative determination of stresses and strains during deformation of nonhomogeneous materials is of great importance. The stress and strain concentrations can be determined quantitatively by experimental or theoretical methods. Experimental determination of the stress-concentration factor generally employs the technique of photoelastic coverings (Ref 6). In Ref 6, this factor has been determined for elastic strains of a matrix containing FeS and SiO_2 inclusions.

Most studies employing the theory of elasticity have been concerned with nonhomogeneous plates (Ref 7), but this is of

J. Pospiech, Research Institute of Ferrous Metallurgy, ul. K. Miraki 12, 44-101 Gliwice, Poland.

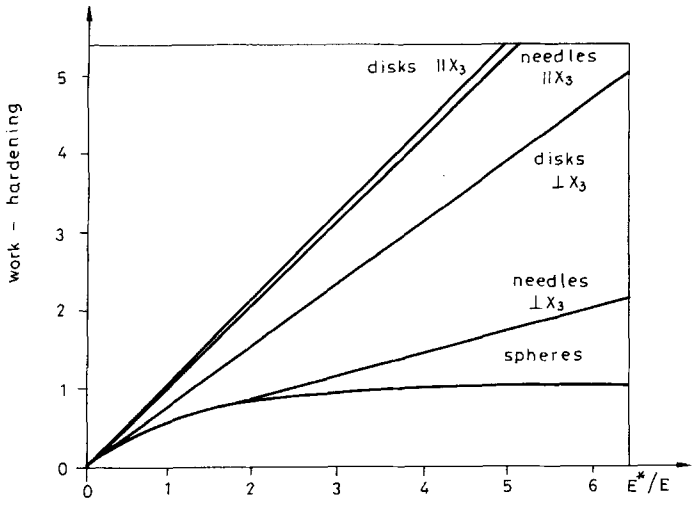

Fig. 1 Influence of inclusion shape on work hardening for 0.01 volume fraction of inclusions. Disks and needles parallel to the tension axis are denoted by $\| x_3$ and those perpendicular to the tension axis by $\perp x_3$. Source: Ref 15

minor interest for plastic-working purposes. Based on the existing solutions in Ref 8, stress concentration has been presented as the function of distance from the interface for the case of the infinite matrix with one particle of the other phase, subjected to uniform uniaxial tension at infinity. This provides information regarding the extent and the magnitude of stress concentration due to the inhomogeneous structure of materials.

Use of the theory of plasticity is normally confined to the formulation and solution of simple cases (Ref 9-12) because of difficulties in the solution of partial differential equations. References 9 to 11 consider the inhomogeneity of materials by assuming that material constants (such as Young's modulus) are functions of the point position. No consideration was given to formation of the secondary state of stress. However, several investigators (Ref 13, 14) have studied the problem of inclusions in a matrix and have calculated concentrations of strains and stresses near inclusions. Argon et al. (Ref 2) have obtained a finite-element solution for the pure shear deformation of an elastic, ideally plastic, nonhardening continuum around a rigid cylindrical inclusion. Spreading of the plastic region with increasing boundary displacements is shown in a set of figures (Ref 2). The author has found one solution that clearly shows generation of the secondary state of stress (Ref 4, 15, 16).

These studies investigate the stress and strain concentrations caused by the presence of variously shaped inclusions by applying the transformation method in tensile testing of cylindrical specimens. It is assumed, among other things, that the matrix undergoes small, uniformly distributed plastic strains: $\varepsilon << 1$ in the direction of axial tension and $-\varepsilon/2$ in perpendicular directions. It is also assumed that inclusions are isotropic and undergo merely elastic strains and that their number is so small that mutual interaction between inclusions can be ignored. Among the most interesting results is the influence of inclusion shape on strain hardening (Fig. 1) (Ref 15). For purposes of this work, it was decided to make use of the case of spheroidal inclusions (often met in practical applications) that transform into ellipsoidal inclusions during deformation. In accordance with Ref 4 and 15, the state of stress in such inclusions, induced by the application of the external stress σ^A_{33} (axis 3 being parallel to the tension axis), is defined as:

$$\sigma^I_{33} = \frac{(7-5\nu)\,E^*\,E\varepsilon}{(7-5\nu)\,(1+\nu^*)E + (8-10\nu)\,(1+\nu)E^*} + \frac{10(1+\nu)\,(1-\nu)E^*\,\sigma^A_{33}}{(7-5\nu)\,(1+\nu^*)E + (8-10\nu)\,(1+\nu)E^*} + \frac{(1-\nu)E^*\,\sigma^A_{33}}{2(1-2\nu^*)E + (1+\nu)E^*} \quad \text{(Eq 1)}$$

$$\sigma^I_{11} = \sigma^I_{22} = -\frac{\sigma^I_{33}}{2} \quad \text{(Eq 2)}$$

where σ^I_{33} is stress in the inclusion, acting in the axis of tension; and σ^I_{11} and σ^I_{22} are stress in the inclusion, acting perpendicular to the axis of tension; E and E^* are the Young's moduli of the matrix and the inclusion, respectively; and ν and ν^* are the Poisson's ratios of the matrix and the inclusion, respectively.

The intensity of shear stresses in the inclusion is defined as:

$$\sigma^I_i = \frac{\sqrt{3}}{2}\sigma^I_{33} \quad \text{(Eq 3)}$$

Equations 1 and 2 confirm the existence of stress and strain concentrations and the generation of the secondary (triaxial) state of stress, which is different from the applied (uniaxial tensile) stress resulting from the material inhomogeneity.

2.2 *Void Growth and Coalescence*

Void growth follows void nucleation. Slow growth of the formed voids follows (Ref 17, 18), and new voids are nucleated during deformation (Ref 19, 20). Crack growth continues until the volume occupied by the cracks reaches a certain boundary magnitude, above which occurs a mutual interaction between the cracks. The cracking process then greatly accelerates as a result of the joining of cracks. It should be remembered that because the nucleation strain is small, and often negligible, the void growth stage is very important in understanding ductile fracture processes in engineering materials (Ref 18).

The Rice and Tracey model (Ref 21) for growth of voids in an infinite material behaving in an ideally plastic manner is described by:

$$\frac{dR}{R} = 0.558\, d\varepsilon^p \cdot \sinh\left(\frac{3}{2}\frac{\sigma_m}{\bar{\sigma}}\right) \quad \text{(Eq 4)}$$

where R is instantaneous void radius, $d\varepsilon^p$ is an increment in equivalent plastic strain, σ_m is hydrostatic stress, and $\bar{\sigma}$ is effective stress. Equation 4 can be integrated between strain values ε^p_1 and ε^p_2 (Ref 22, 23):

$$\ln\left(\frac{R_1}{R_2}\right) = 0.558 \cdot \sinh\left(\frac{\sigma_m}{\bar{\sigma}}\right)\left(\varepsilon_1^p - \varepsilon_2^p\right) \qquad \text{(Eq 5)}$$

where R_1 is void radius at ε_1^p and R_2 is void radius at ε_2^p. Equation 5 can be rearranged and written in terms of void volume (Ref 22):

$$\frac{V_1}{V_2} = \left(\frac{R_1}{R_2}\right)^3 = \exp\left[3 \cdot 0.558 \cdot \sinh\left(\frac{\sigma_m}{\bar{\sigma}}\right)\left(\varepsilon_1^p - \varepsilon_2^p\right)\right] \qquad \text{(Eq 6)}$$

where V_1 is void volume at ε_1^p and V_2 is void volume at ε_2^p. Equation 6 shows a relationship among voids, state of stress, and strains.

A model for the growth of large voids was proposed in Ref 24. Voids are distributed uniformly in an infinite material (matrix). The plane-strain condition is assumed. The solutions of the model were obtained by the elastic-plastic finite-element formulation for large deformation. A result of the computation is shown in a set of figures (Ref 24); deformation is concentrated along the narrow band in the maximum shear stress direction, and the concentration of strain along the band is about two to three times the overall strain for most of the band and about four to five times greater near a large void. Similar results are shown in Ref 25. Voids after nucleation and growth act as stress raisers in the matrix and may cause nucleation of voids at small particles in shear bands, while the particles outside the bands remain relatively inactive (Ref 24).

McClintock (Ref 26) developed a model that consists of a plastically deforming matrix containing a regular array of preexisting cylindrical voids of elliptical cross section, each of which can be envisaged as sitting inside an identical cell. The matrix deforms in generalized plane strain such that the strain parallel to the cylinder axis is uniform but nonzero. The equivalent plastic strain at failure is given by (Ref 26):

$$\bar{\varepsilon}^f = \frac{(1-n)\ln\left(l_0/b_0\right)}{\sinh\left[\frac{1}{2}\sqrt{3}\,(1-n)\left(\frac{\sigma_a+\sigma_b}{\bar{\sigma}}\right)\right] + \frac{3}{4}\left(\frac{\sigma_b-\sigma_a}{\bar{\sigma}}\right)} \qquad \text{(Eq 7)}$$

where σ_a and σ_b are the principal stresses in the remote matrix in the directions of the axes of the voids; l_0 and b_0 are the initial values of hole spacing and semiaxis, respectively; $\bar{\varepsilon}$ and $\bar{\sigma}$ are effective strain and stress; and n is the strain-hardening exponent in the Ludwig power-law relation:

$$\bar{\sigma} = \sigma_0 (\bar{\varepsilon}^p)^n \qquad \text{(Eq 8)}$$

A number of works (Ref 27-36) have analyzed growth and coalescence of voids. The most useful for the purposes of this paper is Ref 32, where numerical solutions for the critical fracture strains ε^f are obtained for uniaxial tension (Lode variable $\nu = +1$) and plane strain tension ($\nu = 0$). The results are plotted against the initial volume fraction of microvoids, V_f, for various values of applied mean-normal stress levels (σ_m/Y), see Fig. 2 and 3 (Ref 32). The results show influence of $\sigma m/Y$, ν (Lode variable), and V_f on ductility.

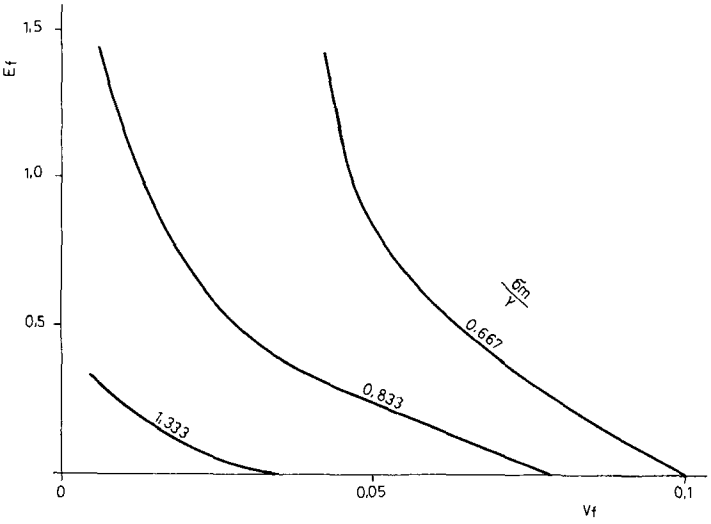

Fig. 2 Theoretical fracture strains for axisymmetric tension ($V = +1$) plotted against the initial volume fraction of microvoids, for various mean-normal stress levels (σ_m/Y). Source: Ref 32

3. Plastic Failure of Carbon Steels

A survey of literature on mechanisms causing cracking of steels as two-phase materials is presented in Ref 37. This paper deals with brittle, plastic, and fatigue failure of steels.

3.1 *Deformation of Cementite*

Schwarz and Blicharski (Ref 38) have reviewed literature on the deformation of cementite.

Most investigations have been concerned with plate-shaped cementite (Ref 40-55) and have employed the electron microscope (Ref 39-42, 44-55). The studies have shown that cementite is plastic mainly above 400 °C (Ref 39-42), but also deforms plastically at room temperature (Ref 39, 40, 43-55). The slightly deformed cementite contained few dislocations; that after greater deformation, dislocation systems and slip bands were formed. Maurer and Warrington (Ref 46) observed an increased dislocation density in plate-shaped cementite after 5% deformation of the specimen, and Inoue et al. (Ref 52) found that the dislocation density of cementite was $2.10^{10}/cm^2$ after rolling the specimen up to 92% of deformation. Slip occurs primarily on (001) and (010) cementite planes (Ref 39, 40, 46, 51, 52). Sometimes, especially above 400 °C, other slip systems become operative. If these systems are unable to compensate for the stresses, the plate-shaped cementite undergoes fracture (Ref 46, 52, 56, 57).

Keh (Ref 39) investigated spheroidal cementite and found that rolling the specimens at room temperature with 50% reduction did not cause distinct deformation of the particles. The deformability of the spheroidal cementite at room temperature was studied using statistical analysis methods (Ref 38). Rolling at room temperature produced a real strain of $\varepsilon_n = 2.85$ (94.2%), which caused a small elongation of the cementite particles (as

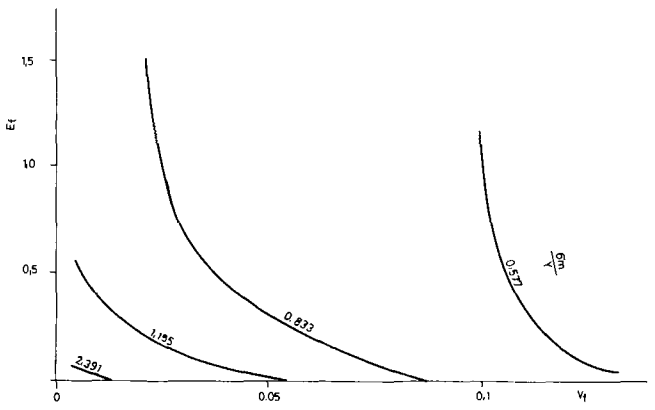

Fig. 3 Theoretical fracture strains for plane-strain tension ($V = 0$) plotted against initial volume fraction of microvoids, for various mean-normal stress levels (σ_m/Y). Source: Ref 32

measured by statistical analysis). This raises doubts as to whether the cementite particles deformed at all, because during rolling these particles, having been elongated after spheroidization, could be rotated. Then only directional alignment of nonequiaxed particles, as noted statistically, would occur. Other investigations have shown that in the case of plate-shaped cementite, thin plates deformed most easily. Thicker plates deformed with greater difficulty and showed a greater tendency to crack (Ref 55).

3.2 *Plastic Failure of Steels Containing Pearlite*

Puttick (Ref 44, 45) investigated the structure, deformation, and tensile failure of eutectoidal steel containing pearlite and minor amounts of ferrite on grain boundaries. The steel contained 0.78% C, which was isothermally transformed at 715 °C. It was found that macroscopic deformation of this steel is caused by slip in the free ferrite and slip in the pearlite grains, the latter being parallel and perpendicular to the cementite lamellae. The slip perpendicular to cementite lamellae may occur as fine slip in particular ferrite plates (joining together later to produce a large deformation) or as "arrowlike" slip. The investigations also demonstrated that slip in the pearlite grains occurs frequently in locations where the cementite lamellae have an incorrect structure resulting from growth faults. The failure of steel proceeds due to cracks perpendicular to the cementite lamellae (in pearlite grains) caused by the transverse slip.

Tipper (Ref 58) determined that the failure of mild steel is caused by cracks in the ferrite that subsequently run through the pearlite. Tipper attached great importance to cracks caused by the presence of nonmetallic inclusions that break their bonds with the matrix (plastic metal). She suggested that the decohesion between a nonmetallic inclusion and the matrix begins after the yield point has been exceeded. She also stated that many cracks caused by the presence of inclusions may be classified erroneously as other types of cracks because some inclusions may be detached during the preparation of microsections. No information was provided regarding the chemical composition, structure, and heat treatment of the investigated steels.

Miller and Smith (Ref 59) extensively studied the mechanisms of steel cracking caused by large plastic strains. Using tensile test specimens, they investigated cracking of a 0.2% C normalized mild steel and demonstrated the occurrence of minor cracks, presumably connected with small inclusions, that play a leading role in the failure of cracks located in pearlite colonies. They also investigated a 0.51% C steel, isothermally transformed at 700 °C to form pearlite. In this steel, failure occurred in the pearlite grains as the result of cracks perpendicular to the cementite lamellae. Measurements made on longitudinal cross sections of the tensile specimens showed that cracks occurred primarily in the pearlite grains with cementite lamellae inclined at 0° to 10° relative to the direction of the tensile stress.

Based on these results, a model of the formation and growth of cracks in pearlite was proposed (Fig. 4) (Ref 59). As a result of the combined action of the tensile stress (as indicated by the relationship between the crystallographic orientation of the cracked pearlite grains and the direction of the tensile stress) and the slip in the free ferrite (Ref 45) or pearlitic ferrite, the crack in the cementite plate presumably occurs at a location of incorrect structure (possibly at a growth fault) (Fig. 4a). This causes a concentration of strain at that location and consequently the formation of further cracks in the neighborhood (Fig. 4b). These local cracks grow and combine (Fig. 4c and d), leading to the formation of one large crack that runs throughout the pearlite grain.

Miller and Smith (Ref 59) also investigated the influence of cementite lamellae thickness in the pearlite grains on the mechanisms of cracking in 0.44% C steel. It appeared that this steel, subjected to isothermal transformation at 692 °C, undergoes failure as a result of pearlite grain cracking. As the temperature of isothermal transformation was decreased, forming finer pearlite, the number of cracked pearlite grains was reduced.

The structure obtained by transformation at 605 °C revealed cracks occurring only in the ferrite (although the micrograph presented suggests the existence of decohesion cracks). This phenomenon was attributed to the reduced thickness of the cementite and ferrite plates produced as a consequence of the lower isothermal transformation temperature (see also Ref 60). Thin cementite lamellae become more resistant to cracking and increase pearlite hardness, thus eliminating the cracking of pearlite grains.

Cracking in carbon steels containing 0.21 to 0.48% C is discussed in Ref 61 and 62. To facilitate the investigation of cracking, a special reagent (nitric acid plus picrin acid plus $FeCl_3 \cdot 6H_2O$ plus ethyl alcohol) was applied, which revealed the microcracks without revealing grain boundaries and slip lines. Takase (Ref 61) investigated carefully the cracking process in 0.48% C steel after complete annealing, normalizing, toughen-

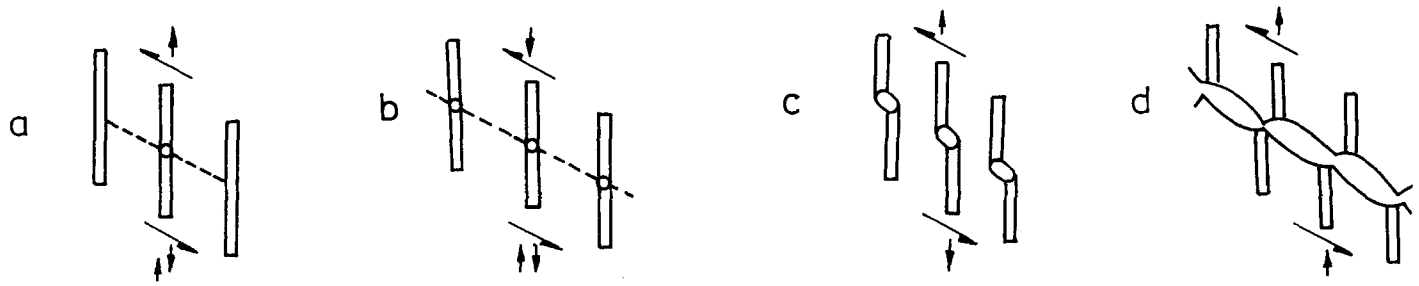

Fig. 4 Development and growth of a pearlite crack. (a) Cracking of one cementite lamella. (b) Cracking of neighboring cementite lamellae due to strain concentration. (c) and (d) Growth and combination of cracks. Source: Ref 59

ing, and softening. Both cracking of pearlite and decohesion occurred in ferrite-pearlite structures; decohesion only was observed in ferrite-spheroidal cementite structures.

Pospiech (Ref 63, 64) investigated the cracking process in 0.38% C steel (35-grade, higher-quality carbon steel) after normalizing using plain tensile specimens. This steel failed due to the generation and development of decohesion cracks (between pearlite and ferrite) and ferrite cracks. Cracks in pearlite were also found.

Inoue and Kinoshita (Ref 65) investigated the deformation and failure of several high-purity steels with carbon contents of 0.39 to 0.91%. All the steels were normalized and strained in a tensile test, and all failed by cracks in pearlite. These cracks can form in two ways. As deformation proceeds, dislocations in the matrix ferrite become operative and motions of dislocation follow in pearlitic ferrite (ferrite lamellae in the pearlite nodule). As the strain of the pearlitic ferrite increases, the stress concentration on the cementite plate increases, eventually leading to microcracking. Once microcracking occurs at one cementite plate, it tends to propagate successively to neighboring cementite plates along the slip direction of the pearlitic ferrite, resulting in the alignment of microvoids. These aligned microvoids are ready to link together and open up to a void as large as the size of a pearlite nodule. In the second mode of crack formation, microvoids initiate preferentially at ferrite/cementite plate interfaces, and aligned microvoids link together by tearing off the cementite to form a void.

Inoue and Kinoshita (Ref 65) found that stages of growth and coalescence of voids associated with pearlite nodules are strongly affected by the volume fraction of pearlite. In steels with lower pearlite contents, voids that form at pearlite nodules link up with one another by means of internal necking of ferrite. The manner of void linkage changes from the internal necking mode to the shearlike mode as the pearlite volume fraction increases.

Barnby and Johnson (Ref 66) investigated the cracking process in 0.48% C steel (after isothermal transformation at 550 °C) and 0.81% C steel (after isothermal transformation at 710 °C) using plain tensile specimens. The pearlite grains revealed both parallel and perpendicular slip in relation to cementite lamellae. In both steels failure was caused by pearlite grain cracking, as a result of cracks perpendicular to the cementite lamellae, produced by transverse slip. The micrographs presented confirm partially that the model proposed by Miller and Smith (Ref 59) is correct.

Danko and Stout (Ref 67) investigated the deformation of 0.8% C steel after isothermal transformation at various temperatures (593, 640, 679, 698, and 704 °C) using impact, tensile, and upset tests carried out at the brittle fracture transition temperature and at higher and lower temperatures. The investigation showed the pearlite to be deformed by kinking. As the temperature of isothermal annealing was lowered, the breadth and the length of kinking in pearlite grains decreased, and the acuity of kinking increased. In all the tests, kinking was the source of cracks.

Lindborg (Ref 68) investigated cracking of 0.86% C steel (caused by plastic deformation) using cylindrical tensile test specimens. The heat treatment of the steel consisted of austenitizing at 900 °C followed by cooling at about 1 °C/min, resulting in rather coarse 0.6 μm thick pearlite plates. Failure mechanisms were investigated at −196, +20, and +200 °C. At 20 °C, kinking in the pearlite and occasional decohesion cracks between the ferrite and cementite were observed. The failure of this steel at 20 °C is caused by cleavage cracks in ferrite, which on reaching the cementite results in cracking of the latter. When a cleavage crack in the ferrite reaches the cementite, some local plastic flow may occur in the ferrite, so that fracture in cementite may follow a cementite cleavage plane for a certain distance and then jump to another cleavage plane, producing a staircase fracture surface with the cementite lamellae. The macroscopic plane of fracture is determined by the cleavage plane of the ferrite. Occasionally, separation in the phase boundary is considerable.

Embury and Fisher (Ref 69) investigated the influence of large amounts of plastic deformation in wire drawing on structure. Among the materials studied was a steel with 0.93% C after isothermal transformation at 670 °C. They found that cementite underwent deformation by slip in those pearlite grains where the cementite lamellae (prior to deformation) were parallel to the direction of drawing. In the remaining grains, bending and fragmentation of cementite occurred.

Plastic deformation in the wire drawing process produced a structure composed of alternately arranged ferrite cells and cells composed of either continuous cementite lamellae (in the case where the same were parallel to the direction of drawing prior to deformation) or fragments of cementite and dislocations (in the case of other orientation of cementite lamellae prior to deformation). A similar cellular structure was obtained in the drawing and forging of 0.004% C bars.

Butcher and Pettit (Ref 70) investigated cracking of eutectoidal 0.78% C steel and three hypereutectoidal steels (0.89, 1.08, and 1.255% C) using tensile test specimens. The heat treatment for 1.255% C steel was chosen so as to obtain a structure composed of pearlite and cementite around the pearlite

grains, but not pearlite and cementite lamellae. For this purpose, the steel was austenitized 1 h at 1000 °C and then isothermally transformed 1 h at 750 °C, followed by furnace cooling. The remaining steels were isothermally transformed at 690 °C. These investigations confirmed that pearlite undergoes deformation by slip parallel and perpendicular to the cementite lamellae. They also confirmed the arrowlike slip.

Results of a study reported in Ref 44 showed that transverse slip occurred primarily at locations of incorrect structure of pearlite (i.e., faults of mismatch type or so-called lines of discontinuity of the cementite lamellae). No deformation by kinking was observed, however. Investigations into the cracking of eutectoid steel have shown the occurrence of cracks perpendicular to the cementite lamellae as well as cracks at other angles in relation to lamellae direction. These cracks were discontinuous; that is, they were small cracks in the cementite lamellae at the front of the main crack, which is in accordance with observations made by van Elst (Ref 71). The occurrence of cracks at boundaries of pearlite grains were not observed.

As the carbon content of steel (beginning at 0.8% C) increases, cracks shift from pearlite grains to the boundaries of pearlite grains. The peak of this phenomenon has been observed in 1.255% C steel. The percentage of crack distribution was as follows: In 0.78% C steel, all the cracks occurred in pearlite; in 1.08% C steel, approximately one-half of the cracks occurred in pearlite and the other half at grain boundaries; and in 1.255% C steel, nearly all the cracks occurred at boundaries of pearlite grains. Two other types of cracks were observed at the pearlite grain boundaries. One type comprises cracks in cementite at grain boundaries parallel to the boundary, caused either by shearing at the ferrite/cementite interface or brittle fracture of cementite. The other type is perpendicular to the cementite layer (at boundaries of pearlite grains). It appears (Ref 70) that the latter type of crack is caused by the process of matching of grain boundaries to the rest of the deformed material, or the condition of providing continuity of the deformed material. It does not appear that these cracks were caused by slip in the adjacent ferrite. Cracks of the second type occur several times more often than cracks of the first type.

3.3 *Plastic Failure of Steels Containing Spheroidal Cementite*

A fundamental and extensive treatment of this subject has been presented by Liu and Gurland (Ref 72), who investigated cracking in eight steels containing from 0.065 to 1.46% C using tensile test specimens. All the steels were hardened and tempered. They were subdivided into two groups, depending on their structure and failure mechanism. Steels of the first group contained 0.065 to 0.3% C, and steels of the second group contained 0.55 to 1.46% C. The cementite nodules were at ferrite grain boundaries in the first group. The mechanism of failure was as follows. Cracks appeared as a result of cracking of cementite nodules and as a result of decohesion between ferrite and cementite. The second stage of cracking involved the growth of decohesion cracks. These two types of cracks linked together and caused macroscopic failure of the specimen.

In steels of the second group, the cementite nodules were much more uniformly distributed in the ferrite. Similar to the steels of the first group, the appearance of cracks due to cracking of the cementite nodules and to decohesion between ferrite and cementite was observed.

The growth of decohesion cracks proceeded analogically in steels of both groups. The main difference was a crack coalescence stage. In the second group, the coalescence of large cracks proceeded due to the appearance of additional, irregular, and noncrystallographic cracks. Such cracks are characterized by the irregular and thorny shape of their fracture lines.

Liu and Gurland (Ref 72) stated that the mode of cracking in steels of the second group is somewhat intermediate between plastic fracture (steels of the first group) and brittle fracture (steels with higher carbon content).

Inoue and Kinoshita (Ref 65) investigated cracking in three steels containing 0.11, 0.40, and 0.39% C using tensile test specimens. The first two steels were commercial-grade plain carbon steels, and the third was a high-purity steel. To obtain spheroidized structures, specimens were quenched and tempered for various times at 700 °C. This treatment produces uniformly distributed carbide particles with average sizes ranging from 0.3 to 1.9 μm. It was shown that in 0.39% C steel, voids form both by decohesion of the carbide/matrix interface and by cracking of carbides with virtually the same frequency. It was also found that void initiation in the 0.39% C steel occurred at a considerably large strain (i.e., at an approximate $\varepsilon = 0.5$), which corresponds to about 40% of the total strain to fracture.

As mentioned previously, Ref 61 and 62 report experimental results regarding fracture of steels containing ferrite and spheroidal cementite. Fracture was caused by decohesion cracks as a result of a broken bond between ferrite and spheroidal cementite.

Pospiech (Ref 63, 64) investigated the cracking process in 0.38% C steel (35-grade, higher-quality carbon steel) after hardening and tempering at 670 °C using plain tensile specimens. The structure of the steel was composed of ferrite fields and generally regular clusters of cementite particles; the latter were characterized by different degrees of coagulation. The steel underwent failure due to generation and growth of decohesion cracks.

Argon and Im (Ref 3, 73) investigated the cracking process in 1045 steel after hardening and tempering using notched tensile specimens. Heat treatment produced nearly equiaxed Fe_3C particles with a volume fraction of 0.125 and a mean particle diameter of 0.44 μm. The steel underwent failure due to generation and growth of decohesion cracks. It was also shown that larger than average size particles separated first and that other particles of smaller diameter separated at progressively larger plastic strains in a certain inverse relation to their size.

In Ref 74, brief mention is made of the failure of a 0.8% C steel after hardening and tempering for 10 days at 650 °C. The diagram shown therein suggests that failure of steel is due to formation and growth of decohesion cracks, although it is reported in the text that cracks resulting from the cracking of cementite nodules also occur.

Gurland (Ref 75) investigated the cracking process in a spheroidized carbon tool steel (1.05% C, 0.20% Mn, and 0.20% Si) deformed at room temperature under various loading conditions. In tension, the average size of the broken particles was larger than the average size of all particles, and cracking occurred preferentially in particles oriented with their longest

axis parallel to the direction of the tensile stress. During deformation in tension, compression, or torsion, the orientation of cracks initiated in particles tended to be perpendicular to the direction of the maximum tensile strain. The investigation also showed that it is possible to eliminate cracks through heat treatment. This last point is especially interesting.

4. Conclusions

This paper reviews the research work devoted to the deformation and fracture of steels containing cementite. The deformability of steels depends primarily on the number, properties, and distribution of second-phase particles. During deformation, the presence of second-phase particles in the plastic matrix causes generation of other states of stress and the concentration of stress and strain. Local concentrations of stress and strain, growing with macroscopic deformation, cause local cracking, which, in combination with the second-phase particles, results in the formation of a new state of stress and new concentrations of stress and strain. This causes new microcracks to grow and coalesce, resulting in macroscopic fracture of the material.

This paper also reviews work devoted to the deformation and fracture of carbon steels in plastic cold-working processes. Worthy of special attention is the possibility, presented in one work, of healing the microcracks produced by deformation, by means of appropriate heat treating processes.

Acknowledgments

The author expresses his thanks to Prof. Dr. R. Wusatowski (the promoter of the author's Ph.D. thesis, of which this paper is a part), Dr. K. Rytel, Mrs. G. Wiszniewska, Mrs. H. Bocianowska, Mrs. H. Koniczek, Mrs. M. Adamowicz, Mrs. I Grygiel, and Mr. U. Sierankowska for their assistance in performing this work.

References

1. J. Pospiech, *Prace IH*, Vol 26 (No. 3), 1974, p 159
2. A.S. Argon, J. Im, and R. Safoglu, *Metall. Trans. A*, Vol 6A (No. 4), 1975, p 825
3. A.S. Argon, *J. Eng. Mater. Technol. (Trans. ASME)*, Vol 98 (No. 1), 1976, p 60
4. K. Tanaka, T. Mori, and T. Nakamura, *Philos. Mag.*, Vol 21 (No. 170), 1970, p 267
5. K. Takase, private communication, Yokohama, Japan, 1985
6. W.M. Finkel and O.P. Jeliesina, *Metalloved. Term. Obrab. Met.*, Vol 7, 1971, p 55
7. E.M. Saleme, *J. Appl. Mech.*, Vol 25 (No. 1), 1958, p 129
8. J. Gurland and J. Plateau, *Trans. ASM*, Vol 56, 1963, p 442
9. W. Olszak, *Arch. Mech. Stos.*, Vol 6 (No. 3), 1954, p 493
10. W. Olszak, *Arch. Mech. Stos.*, Vol 6 (No. 4), 1954, p 639
11. J. Nowinski, *Arch. Mech. Stos.*, Vol 6 (No. 4), 1954, p 665
12. W. Olszak, J. Rychlewski, and W. Urbanowski, *Adv. Appl. Mech.*, Vol 7, 1962, p 131
13. W.C. Huang, *Int. J. Solids Struct.*, Vol 8, 1971, p 149
14. J. Orr and D.K. Brown, *Eng. Fract. Mech.*, Vol 6, 1974, p 261
15. K. Tanaka and T. Mori, *Acta Metall.*, Vol 18 (No. 8), 1970, p 931
16. K. Tanaka, K. Wakashima, and T. Mori, *J. Mech. Phys. Solids*, Vol 21 (No. 4), 1973, p 207
17. Y.W. Shi and J.T. Barnby, *Int. J. Fract.*, Vol 25, 1984, p 143
18. J.T. Barnby, Y.W. Shi, and A.S. Nadkarni, *Int. J. Fract.*, Vol 25, 1984, p 273
19. J. Gurland, *Acta Metall.*, Vol 20 (No. 5), 1972, p 735
20. T.B. Cox and J.R. Low, *Metall. Trans. A*, Vol 5A (No. 6), 1974, p 1457
21. J.R. Rice and D.M. Tracey, *J. Mech. Phys. Solids*, Vol 17 (No. 3), 1969, p 201
22. J.T. Barnby, Y.W. Shi, and A.S. Nadkarni, *Structural Failure, Product Liability and Technical Insurance, Proc. 1st Int. Conf.*, (Vienna), H.P. Rossmanith, Ed., Elsevier Science Publishers B.V. North Holland, 1984, p 219
23. Y.W. Shi, J.T. Barnby, and A.S. Nadkarni, *6th Int. Conf. Fracture*, S.R. Valluzi et al., Ed., Pergamon Press, Oxford, 1984, p 1329
24. S.I. Oh, C.C. Chen, and S. Kobayashi, *J. Eng. Ind. (Trans. ASME)*, Vol 101 (No. 1), 1979, p 36
25. J.W. Hancock and A.C. Mackenzie, *J. Mech. Phys. Solids*, Vol 24 (No. 2/3), 1976, p 147
26. F.A. McClintock, *J. Appl Mech.*, Vol 35, 1968, p 363
27. P.F. Thomason, *J. Inst. Met.*, Vol 96 (No. 12), 1968, p 360
28. P.F. Thomason, *Acta Metall.*, Vol 29 (No. 5), 1981, p 763
29. P.F. Thomason, *Acta Metall.*, Vol 30 (No. 1), 1982, p 279
30. P.F. Thomason, *Rev. Metall.*, No. 5, 1983, p 233
31. P.F. Thomason, *Acta Metall.*, Vol 33 (No. 6), 1985, p 1079
32. P.F. Thomason, *Acta Metall.*, Vol 33 (No. 6), 1985, p 1087
33. A.L. Gurson, *J. Eng. Mater. Technol. (Trans. ASME)*, Vol 99 (No. 1), 1977, p 2
34. V. Tvergaard, *J. Mech. Phys. Solids*, Vol 30, 1982, p 265
35. V. Tvergaard, *Int. J. Fract.*, Vol 17, 1981, p 389
36. V. Tvergaard, *Int. J. Fract.*, Vol 18, 1982, p 237
37. A.R. Rosenfield, G.T. Hahn, and J.D. Embury, *Metall. Trans.*, Vol 3(11) 1972, p 2797
38. A. Schwarz and M. Blicharski, *Hutnik*, No. 6, 1985, p 204
39. A.S. Keh, *Acta Metall.*, Vol 11, 1963, p 1101
40. A. Inoue, T. Ogura, and T. Masumoto, *Metall. Trans. A*, Vol 8A (No. 11), 1977, p 1689
41. I.N. Bogaczew and T.S. Wietrowa, *Izv. V.U.Z. Tsvetn. Metall.*, Vol 12, 1975, p 111
42. A.A. Ryzikow and W.I. Rulew, *Izv. V.U.Z. Tsvetn. Metall.*, Vol 3, 1982, p 113
43. R.F. Campbell, *Trans. ASM*, Vol 40, 1948, p 954
44. K.E. Puttick, *J. Iron Steel Inst.*, Vol 185 (No. 2), 1957, p 161
45. K.E. Puttick, *J. Iron Steel Inst.*, Vol 185 (No. 2), 1957, p 167
46. K. Maurer and D.H. Warrington, *Philos. Mag.*, Vol 15, 1967, p 321
47. D.F. Lupton and D.H. Warrington, *Met. Sci. J.*, Vol 6, p 200
48. D. Goodchild, *Scand. J. Met.*, Vol 1, 1972, p 235
49. B. Karlsson and G. Linden, *Mater. Sci. Eng.*, Vol 11, 1975, p 209
50. B. Karlsson and G. Linden, *Mater. Sci. Eng.*, Vol 17, 1975, p 153
51. J. Gil Sevillano, *Mater. Sci. Eng.*, Vol 21 (No. 3), 1975, p 221
52. A. Inoue, T. Ogura, and T. Masumato, *Trans. Jpn. Inst. Met.*, Vol 17, 1976, p 149
53. A. Inoue, T. Ogura, and T. Masumoto, *Scr. Metall.*, Vol 11 (No. 1), 1977, p 1
54. Y. Kurita and L. Roesch, *Mem. Sci. Rev. Metall.*, Vol 74, 1977, p 731
55. G. Langford, *Metall. Trans. A*, Vol 8A, 1977, p 861
56. G. Langford, *Metall. Trans.*, Vol 1, 1970, p 465
57. V.K. Chandhok, A. Kasak, and J.P. Hirth, *Trans. ASM*, Vol 59, 1966, p 288
58. C.F. Tipper, *Metallurgia*, Vol 39 (No. 231), 1949, p 133
59. L.E. Miller and G.C. Smith, *J. Iron Steel Inst.*, No. 11, 1970, p 998
60. J.A. Rinebolt, *Trans. ASM*, Vol 46, 1954, p 1527

61. K. Takase, *Proc. Int. Conf. Strength of Metals and Alloys* (Tokyo), Vol 9. Japan Institute of Metals, 1968, p 862-867
62. K. Takase and Y. Kurita, *Proc. ICSTIS, Suppl. Trans. Iron Steel Inst. Jpn.*, Vol 11, 1971, p 862-867
63. J. Pospiech, *J. Mech. Work. Technol.*, Vol 12, 1985, p 93
64. J. Pospiech, Ph.D. thesis, Research Institute of Ferrous Metallurgy, Gliwice, Poland, 1978
65. T. Inoue and S. Kinoshita, *Trans. Iron Steel Inst. Jpn.*, Vol 17 (No. 9), 1977, p 523
66. J.T. Barnby and M.R. Johnson, *Met. Sci. J.*, No. 7, 1969, p 155
67. J.C. Danko and R.D. Stout, *Weld. J. Suppl.*, No. 3, 1955, p 113s-116s
68. U. Lindborg, *Trans. ASM*, Vol 61, 1968, p 500
69. J.D. Embury and R.M. Fisher, *Acta Metall.*, Vol 14, 1966, p 147
70. B.R. Butcher and H.R. Pettit, *J. Iron Steel Inst.*, Vol 204 (No. 5), 1966, p 469
71. H.C. Van Elst, *Trans. AIME*, Vol 230, 1964, p 460
72. C.T. Liu and J. Gurland, *Trans. ASM*, Vol 61, 1968, p 156
73. A.S. Argon and J. Im, *Metall. Trans. A*, Vol 6A (No. 4), 1975, p 839
74. T. Gladman, B. Holmes, and I.D. McIvor, *Effect of Second-Phase Particles on the Mechanical Properties of Steel*, Iron and Steel Institute, London, 1971, p 68-78
75. J. Gurland, *Acta Metall.*, Vol 20 (No. 5), 1972, p 735